Numerical analysis of energy piles under different boundary conditions and thermal loading cycles

Ali Khosravi[1,a], Aria Moradshahi[2], John S. McCartney[3], and Mirmohammadreza Kabiri[4]

[1] *Assistant Professor, Civil Engineering Department, Sharif University of Technology, Tehran, Iran*
[2] *Graduate Student, Civil Engineering Department, Sharif University of Technology, Tehran, Iran*
[3] *Associate Professor, Department of Structural Engineering, University of California San Diego, La Jolla, USA*
[4] *Ph.D., Dept. of Civil, Environmental, and Architectural Engineering, Univ. of Colorado Boulder, Boulder, USA*

Abstract. The thermo- mechanical behavior of energy piles has been studied extensively in recent years. In the present study, a numerical model was adapted to study the effect of various parameters (e.g. heating/cooling temperature, head loading condition and soil stiffness) on the thermo-mechanical behavior of an energy pile installed in unsaturated sandstone. The results from the simulations were compared with measurements from a thermal response test on a prototype energy pile installed beneath a 1-story building at the US Air Force Academy (USAFA) in Colorado Springs, CO. A good agreement was achieved between the results obtained from the prototype and the numerical models. A parametric evaluation were also carried out which indicated the significance of the stiffness of the unsaturated sandstone and pile's head loading condition on stress-strain response of the energy pile during heating/cooling cycles.

1 Introduction

In recent years, reinforced concrete piles have been widely used as geothermal heat exchangers to access the relatively constant temperature of the ground for efficient heating and cooling of buildings [1-15]. Deformation in energy piles is a complex process due to interaction between soil and pile and the effects of temperature change on the thermal expansion and contraction of the pile and surrounding subsurface. Deformations in this case may occur due to initial mechanical loading associated with construction of the overlying building, and thermo-elastic expansion and contraction of the reinforced concrete during heating and cooling, as well as settlement or heave of the surrounding subsurface.

Reviewing the literature, it was found that some aspects of soil-pile behavior have gained less attention than their actual impact in energy piles. Considering the fact that a pile foundation may be subjected to different vertical loads, it is essential to consider the effect of overlying structures on thermo-mechanical response of an energy pile. Additionally, strength properties of soil surrounding the pile seems to have an influence on lateral and axial deformations [17-21]. This study seeks to examine these two aspects by means of a 2D finite difference analysis to predict the deformation behavior of an energy pile during thermo-mechanical loading.

First, the model was validated based on the results from a series of comprehensive full-scale in-situ tests, investigating the behavior of eight energy piles installed beneath a one-story building at the US Air Force Academy (USAFA) in Colorado Springs, CO. Pile deformations were then evaluated at different temperatures during active heating and ambient cooling. Finally, a parametric study was carried out to examine the effects of different head conditions and surrounding soil strength characteristics followed by a discussion on obtained results.

2 Case study energy pile

2.1 Pile description and instrumentation

The case pile is an energy pile with a circular section of diameter, D, of 0.61 m and length, L, of 15.6 m which was selected from an energy pile testing research project at the Field Engineering and Readiness Laboratory (FERL) of the US Air Force Academy (USAFA), Colorado Springs, CO (Pile 4 in Fig. 1). This pile was part of a supporting system of eight drilled shaft energy piles which were used to support a one-story building. The Young's modulus and coefficient of thermal expansion of the foundation were reported to be 30 GPa and 13 με/°C respectively [12].

The soil profile of the site together with the geometry of the pile, and embedded instrumentation are presented in Figure 2. As presented in this figure, the top layer of the soil system consists of a layer of medium dense, sandy fill with silt and gravel, having a thickness of 1 m

[a] Corresponding author: khosravi@sharif.edu

and a dry unit weight of 18.4 kN/m^3. The second layer is an approximately 1 m thick medium dense sandy-silty gravel layer having a dry unit weight of 19.2 kN/m^3. Below the second layer is Dawson–Arkose bedrock (sandstone), from a depth of approximately 2 m below the surface to the maximum depth of investigation. The foundation unit weight is 25 kN/m^3. The water table was considered to be at a depth greater than 16 m based on the results of exploration.

Different instrumentation was incorporated into the energy pile to investigate the axial strain and stress behavior of the piles during thermo-mechanical loading. Distribution of axial strain of the pile with depth was measured using a set of twelve Geokon Model 4200 vibrating wire strain gauges (VWSGs) (Fig. 2). A series of ten Geokon model 3810 thermistor strings were also used for monitoring temperature variations in the soil surrounding the energy pile.

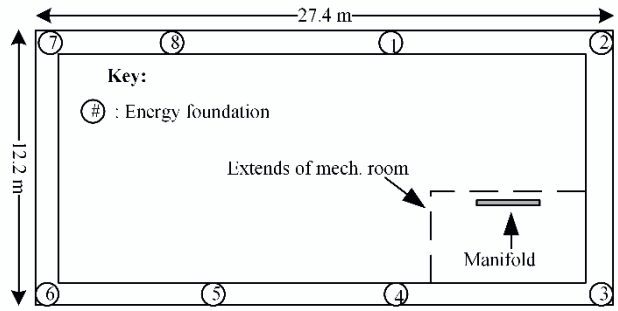

Figure 1. Schematic of the location of the energy piles under the building

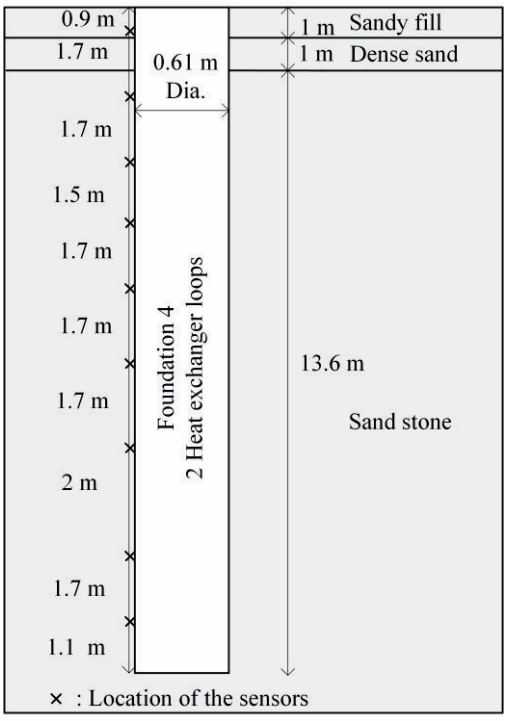

Figure 2. Schematic of soil layers and foundation instrumentation for Foundation 4

Different cycles of heating and cooling were imposed to the foundation using a heating system consisting of a series of loops of HDPE heat exchanger tubing with an average diameter of 20 mm attached to the inside part of the reinforcing cages of the foundations, and a heating unit to heat and circulate a 20 % propylene glycol–water mixture through the heat exchanger loops. More details about the heating system are presented in [16].

The thermal loading process included an initial heating of the foundation for approximately 498 hours, after which fluid circulation in the foundation was stopped and the cooling process began for almost 700-1200 hours. During the heating and cooling cycles, thermo-mechanical behavior of the foundation was obtained for times corresponding to foundation temperature average changes of 6 °C. The profiles of foundation temperature are presented in Figure 3. As shown in this figure, variations in temperature with depth is relatively constant, except for depths below 11 m, where slight changes in the temperature were observed with depth.

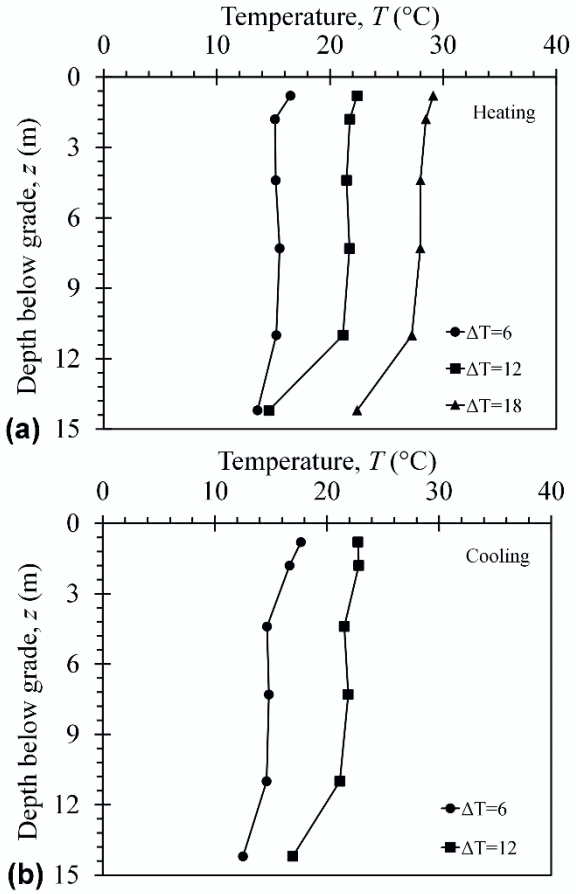

Figure 3. Profiles of foundation temperatures during different cycles of (a) heating; (b) cooling

2.2 Numerical model description

A finite difference method was adopted to simulate an axisymmetric model for energy pile analysis during subsequent cycles of heating and cooling, using the finite difference code FLAC^{2D} version 4. The finite difference method has been reported to be an efficient way to analyze the behavior of energy piles, [8], as it considers complexities arising from boundary conditions, thermo-hydro-mechanic loading, geometry, soil properties and so forth in solving equations that are related to thermo-

hydro-mechanical problems. The model and its mesh discretization are presented in Figure 4. As shown in this figure, except a 1 m dense sand overlain by a 1 m sandy fill along the shaft, rest of surrounding soil is unsaturated mostly sandstone. The boundary distances in horizontal and vertical directions, from shaft and pile tip are 10 m and 25 m in the axisymmetric model, respectively. Due to high stress gradients near the pile shaft, smaller mesh dimension were adopted around the pile (25×25 cm within 5 m from the shaft) than those outside this zone. The Mohr-coulomb failure criterion was used for the geomaterial and a fully linear elastic behavior was considered for the energy pile. The properties of the materials used in this study are presented in Tables 1 and 2.

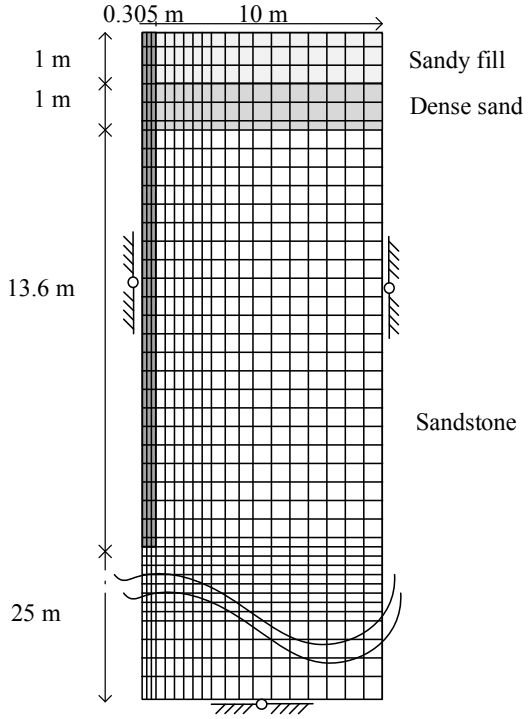

Figure 4. Geometry and 2D mesh discretization of the model

Table 1. Properties of the model

	Sandy fill	Dense sand	Sandstone	Foundation
Bulk Mod. (MPa)	60	90	200	15000
Shear Mod.(MPa)	22.5	33.75	67.55	6500
Thermal conductivity (W/m°C)	1.11	0.8	1.233	1.8
Specific heat extraction (J/kg°C)	800	700	800	900
Coefficient of thermal expansion ($\times 10^{-6}$ J/°C)	6	5	6	13
Poisson's ratio	0.3	0.25	0.2	0.2

Table 2. Properties of the soil-pile interfaces

	Sandy fill	Dense sand	Sandstone
Normal stiffness (MN/m^3)	140	200	450
Shear stiffness (MN/m^3)	50	120	350
Cohesion (kPa)	100	50	0
Friction (°)	20	30	35

To analyze the thermal behavior of the energy pile, the pile was initially subjected to a vertical mechanical load of about 300 kN due to the dead weight of the building. The energy pile was then subjected to different cycles of temperature changes of ±19°C from an initial temperature of 10°C which is the reported mean ground temperature. Figure 5 shows the thermal loading path considered for the analysis. As shown in this figure, two subsequent cycles of heating and cooling were applied to the pile. During each cycle, the pile temperature was elevated to an average temperature of 29°C from a ground temperature in 500 h and then decreased to the ground temperature in 1200 h.

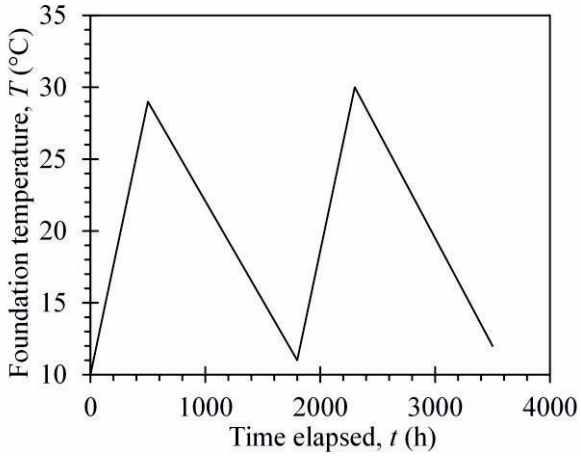

Figure 5. Thermal loading path for two cycles of heating and cooling

3 Results

Figures 6 and 7 demonstrate the results of the analyses in terms of thermal axial strain (Fig. 6a) and stress (Fig. 6b) against depth during heating and cooling cycles, respectively. The filed measurements reported by [12], were also presented in these two figure for comparison purposes. As can be observed, the model provided profiles of stress and strain very similar to in-situ trends at different temperatures. Based on the results presented in these figures, the thermal axial strains became more negative with temperature increase, indicating the expansion of the pile during heating. While during cooling cycles, the thermal axial strains were reduced, showing a contraction trend in the pile. The thermal axial strain profiles of both in-situ and numerical analyses have relatively consistent shapes at different temperatures. As

a result of soil–structure interaction, due to the mobilization of shear resistance along sides of the foundation, a nonlinear distribution in thermal strain was observed with depth similar to reports from [2] and [14]. The thermal axial strain profiles showed an initial decrease in magnitude with depth to a depth of about 9 m (the location of the null point), followed by axial strain increase at greater depths. The thermal axial stress experienced an initial increase with depth to a maximum value at a depth of 8-10 (the null point). The stress appeared to decrease at greater depths. The same trends for axial strain and stress with depth were observed during both heating and cooling cycles.

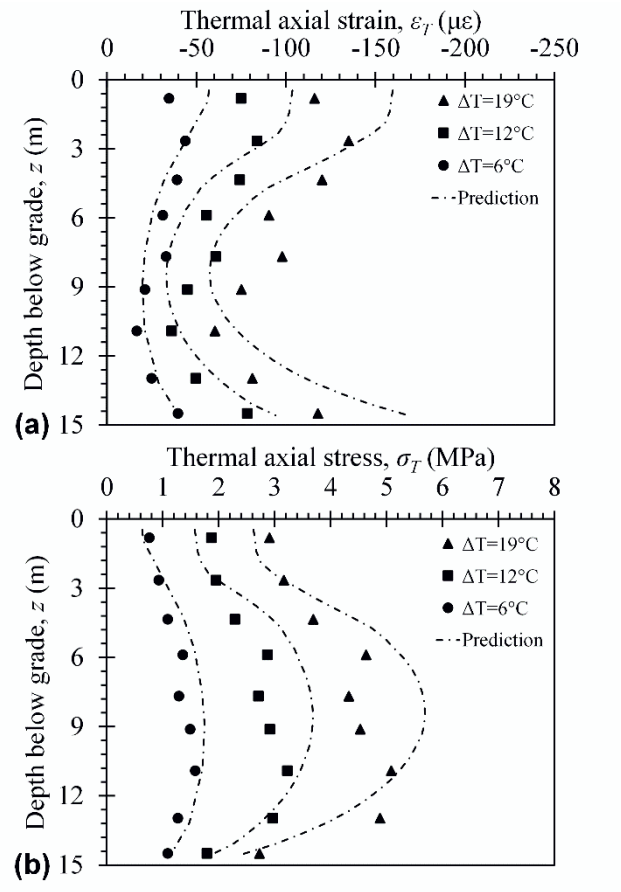

Figure 6. Thermal axial (a) strain; (b) stress; for heating to different temperatures

Thermally induced displacements of the energy pile during heating and cooling cycles are shown in Figure 8. Based on results presented in this figure, for depths above the null point, the pile would experience an upward movement during heating with an uplift in the surface, while the lower part of the pile would experience expansion with a downward movement. During cooling, the behavior was totally different. The energy pile tends to contract above the null point and upper portions of the pile were moving downward while lower parts were moving upward resulting in settlement of the surface. Additionally, as observed in Figure 9, the magnitudes of vertical displacement decreases during the second cycles of heating and cooling.

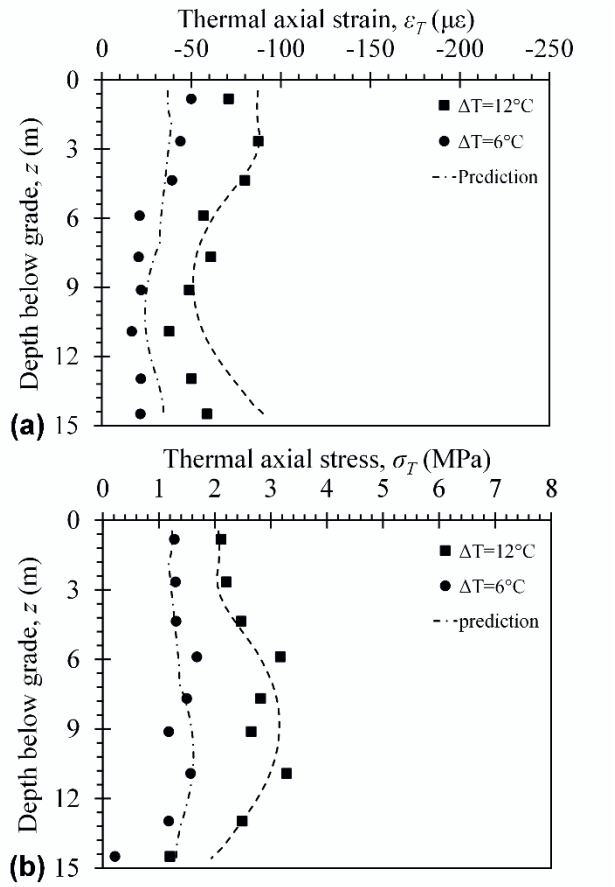

Figure 7. Thermal axial (a) strain; (b) stress; for cooling to different temperatures

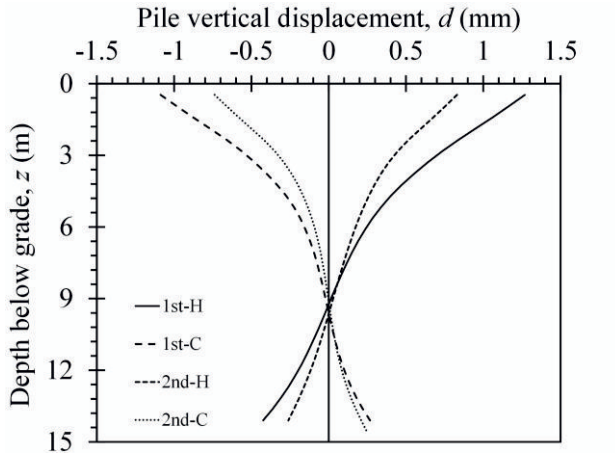

Figure 8. Pile displacement values for heating and cooling cycles

Figure 9 provides the mobilized side shear stresses measured along the soil-pile interface for different cycles of heating and cooling. During the heating cycle, at upper part of the pile lower magnitudes of shear stress were observed while at lower part, higher shear stresses were mobilized. Side shear stresses during the cooling cycle show significantly lower values. The point at which the sign of the mobilized side shear stress changes, shows the location of the null point where the axial thermal stress and strain are maximum and minimum respectively.

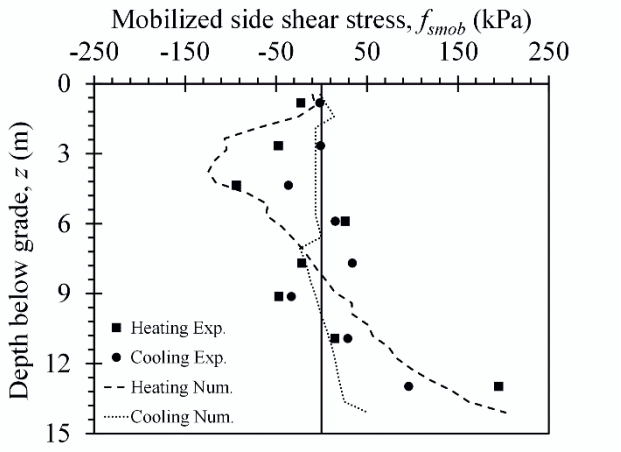

Figure 9. Mobilized side shear stress

4 Parametric evaluation

A parametric evaluation was performed in this study to explore the effect of head-structure stiffness and soil properties on the behavior of an energy pile. The impact of overlying structure was investigated by applying vertical loads, p, with different magnitudes to the pile head, and the stiffness of the surrounding soil was assessed through changing soil's Young modulus, E, of the sandstone layer.

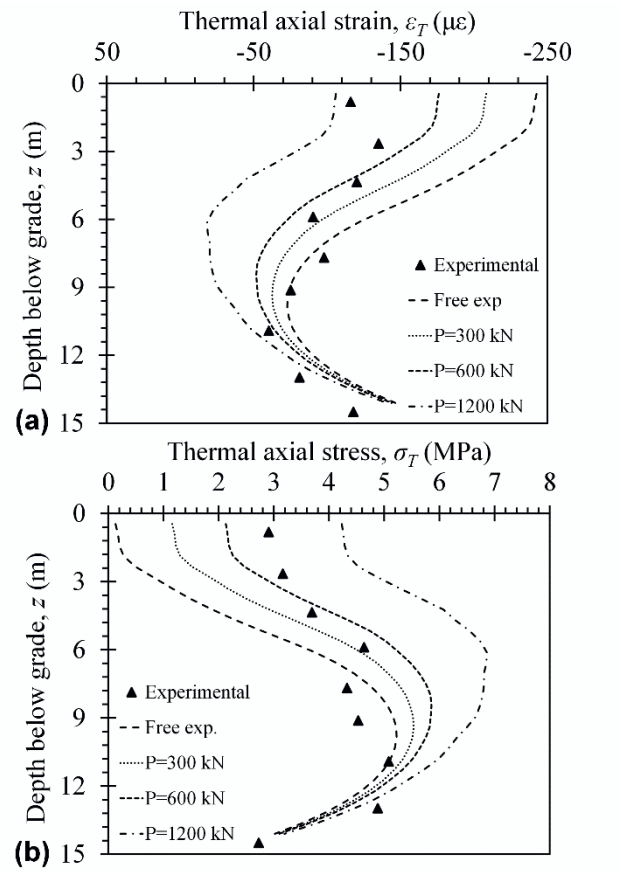

Figure 10. Thermal axial (a) strain; (b) stress; for heating and different weight of the building for heating to 19°C

4.1 Effect of different head loading conditions on pile behavior

The impact of head loading condition on the response of energy piles was investigated in this study by performing an evaluation process of four different values of vertical load. Results of the evaluation process are presented in Figure 10. In this figure, the data points represent the measured in-situ data for a pile without a vertical load and the dashed lines are the predicted stress/strain values.

As presented in this figure, by increasing the vertical load applied to the pile head, a larger thermal axial stress was observed at the top of the pile, while the profiles of strain shifted to the left. The rate of changes in the thermal axial stresses and strains with the load of overlying structure was also different through the depth. For the values of p of 0 to 1200 kN, axial strain at the pile head would range from -250 to -110 με, while no change would happen at the toe where the behavior was mostly controlled by the stiffness of the underlying soil.

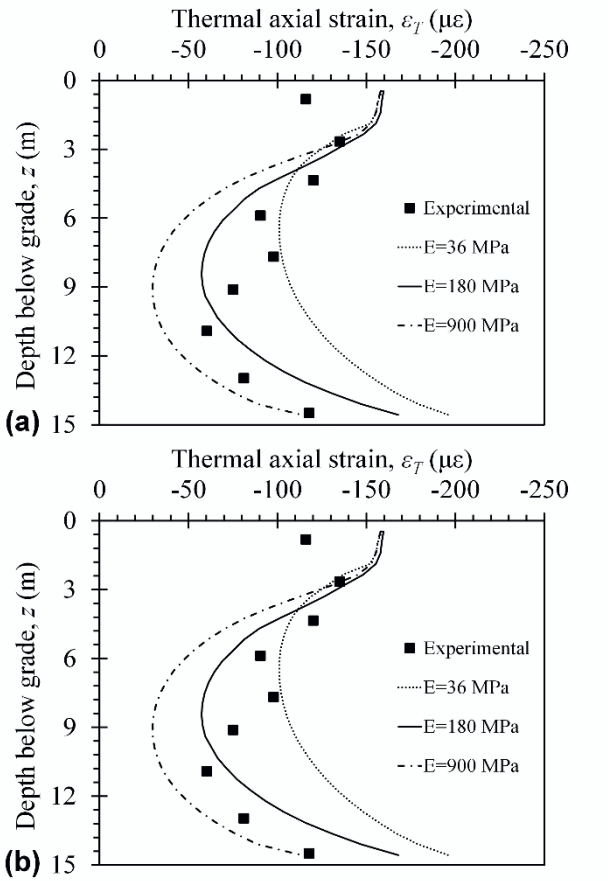

Figure 11. Thermal axial stress and strain profiles for different stiffness of surrounding soil

Based on the results of numerical modeling, the maximum thermal axial stress for the pile that was subjected to p=1200 kN was about 6.8 MPa which was in good agreement with the value of 6.45 MPa reported by [16]. It is clear from this figure that the null point moved upward as the head restraint was increased.

4.2 Effect of surrounding soil stiffness on pile behavior

Results for axial stress and strain are presented in Figure 11 for different values of Young's modulus of the surrounding soil (36 MPa, 180 MPa, and 900 MPa). As observed in this figure, the resistance of the surrounding soil may have a significant influence on the distribution of the thermal axial stress and strain profiles which is almost similar to the effect of overlying structure. As the value of the Young's modulus of the soil increased, higher thermal axial stress and lower thermal axial strain were observed.

5 Conclusion

Energy piles are important elements since they function as load-bearing elements while they are capable of providing thermal energy for buildings. Heating and cooling cycles due to seasonal fluctuations in temperature, weight of the overlying structure, and stiffness of the surrounding soil play important role in affecting the thermo-mechanical behavior of energy piles.

A numerical simulation was conducted using finite difference method to investigate the thermo-mechanical behavior of the energy piles. The study considered different conditions for temperature, head-restraint, and soil stiffness to provide a comprehensive understanding of the factors affecting the pile response. The results of the study proved that, heating and cooling cycles significantly affect the distribution of thermal axial stress and strain. Also during heating cycle, the pile was observed to expand and surface uplift was observed, while during cooling cycle the surface settled due to contraction of the pile. The measured deformations were lower in second cycles of heating and cooling. The study also indicated that the effect of the overlying structure and the surrounding soil stiffness are similar. Increasing the weight of the structure and stiffness of the soil results in higher values for thermal axial stress and lower values for thermal axial strain. The results of the numerical study was completely in agreement with the observed response of a case study energy pile at the US Air Force Academy (USAFA) in Colorado Springs, CO.

Acknowledgement

J. McCartney would like to thank the support from DoD ESTCP project EW-201153 and NSF project CMMI-0928159. The views in this paper are those of the authors alone.

References

1. K.D. Murphy, J.S. McCartney, K.S. Henry, Acta Geotechnica. **10**(2), 179-195 (2015)
2. L. Laloui, M. Nuth, L. Vulliet, Int. J. Nem. Anal. Meth. Geomech. **30**, 763-781 (2006)
3. M.E. Suryatriyastuti, H. Mroueh, S. Burlon, Com. And Geotech. **55**, 378-391 (2014)
4. B.L. Amatya, K. Soga, P.J. Bourn-webb, T. Amis, L. Laloui, Geotech. **62**(6), 503-519 (2012)
5. D. Adam, R. Markiewicz, Geotech. **59**(3), 229-236 (2009)
6. S. O'Connell, S.F. Cassidy, Int. Geoth. Con. *Reykjavik*, 12-18 (2003)
7. H. Brandl, Geotech. **56**(2), 81-122 (2006)
8. M.E. Suryatriyastuti, H. Mroueh, S. Burlon, Renew. And Sust. Ene. Rev. **16**, 3344-3354 (2012)
9. T. Mimouni, L. Laloui, Acta Geotech. **9**(3), 355-366 (2014)
10. L. Laloui, A. Di Donna, *Proceeding of the ICE-Civil. Eng.* **64**(4), 184-191 (2011)
11. C. Knellwolf, H. Peron, L. Laloui, J. Geotech, Geoenviron. Eng. **137**(12), 890-902 (2011)
12. J.S. McCartney, K.D. Murphy, DFI. J. **6**(2), 28-36 (2012)
13. J. Gao, X. Zhang, J. Liu, K. Li, J. Yang, Appl. Ene. **85**(10), 901-910 (2008)
14. P.J. Bourne-Webb, B. Amatya, K. Soga, T. Amis, C. Davidson, P. Payne, Geotech. **59**(3), 237-248 (2009)
15. W. Wang, R. Regueiro, J.S. McCartney, Geotech. and Geolog. Eng. **33**(2), 373-388.
16. K.D. Murphy, J.S. McCartney, Geotech. and Geolog. Eng. **33**(2), 343-356 (2015)
17. C.G. Olgun, T.Y. Ozudogru, S.L. Abdelaziz, A. Senol, Acta Geotech. **10**(5), 553-569 (2014a)
18. C.G. Olgun, J.S. McCartney, J. Deep piles Inst. **8**(2), 58-72 (2014)
19. C.J. Wood, H. Liu, S.B. Riffat, Geotech. **59**(3), 287-290 (2009)
20. O. Ghasemi-Fare, P. Basu, Ene. and Buil. **66**, 470-479 (2013)
21. K.D. Murphy, J.S. McCartney, Geotech. and Geolog. Eng. **33**(2), 343-356 (2015)